Journal of Materials Chemistry A

Accepted Manuscript

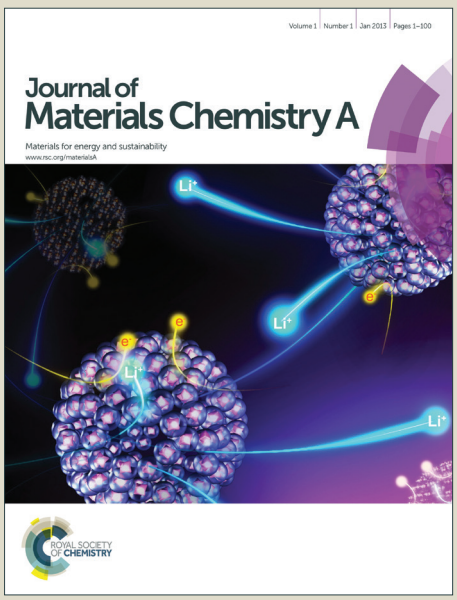

ROYAL SOCIETY OF CHEMISTRY

www.rsc.org/materialsA

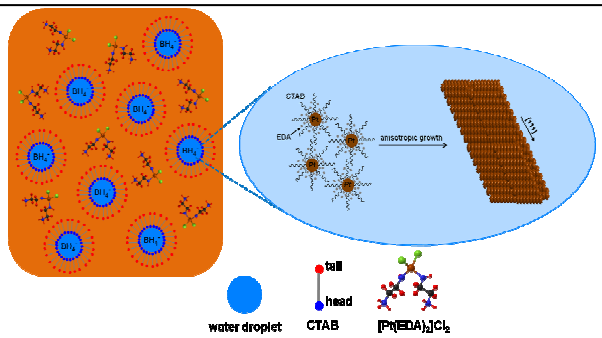

Novel platinum nanobelts were synthesized using a reverse micelle method for the first time. Morphology control over the shape and size of the nanobelts can be done simply by changing the precursor concentration or reaction time.

Journal of Materials Chemistry A RSCPublishing

COMMUNICATION

Shape Control of Novel Platinum Nanobelts

Cite this: DOI: 10.1039/x0xx00000x

Y. Liu,[a,b] S. Poyraz,[a] J. H. Xin[b] and X. Zhang*[a]

Received 00th January 2012,
Accepted 00th January 2012

DOI: 10.1039/x0xx00000x

www.rsc.org/

Novel platinum nanobelts were synthesized using a reverse micelle method for the first time. Morphology control over the shape and size of the nanobelts can be done simply by changing the precursor concentration or reaction time. The nanobelts show high electrocatalytic activity and tunable surface properties, indicating their high application potential in catalyst, sensor and fuel cells.

With the possibility of establishing higher performance system with lower material utilization and enhanced efficiency, the nanoscale materials have raised substantial research attention within decades. Compared to their bulk counter-part, the nanoscale materials would have different properties originated from: (i) the electronic motion confinement in the nano-length scale; (ii) anisotropic surface wettability for various shapes and facets; and (iii) exponential increment in surface area. As a result, a nanostructured material may have distinct optical (e.g. surface plasmon resonance), catalytic, and thermodynamic properties. On the other hand, by controlling the shape and size of the nanomaterials, the correlation between shape/size and chemophysical property can be revealed, where an advanced nano-engineering system can also be structured and designed.

The nanostructured metals, metal oxides, and ceramics have received extensive research effort within decades, due to their unique optical, chemical or electronic properties; as well as their potential wide-spread application in field-effect transistors, electrocatalysis and fillers.[1] Among the myriad of these conductive or semiconducting materials, special attention is paid to the nanoscale platinum (Pt) materials resulting from their distinct catalytic property and chemical stability.[2] Pt nanostructures of different shapes have been vastly synthesized, such as nanospheres (0D), nanowires (1D), nanodendrites (3D), nanocubes, and nanodisks; which also demonstrate notable surface-enhanced plasmon resonance, sensory, and electronic properties.[3] However, there is no recent report on the synthesis of the quasi-1D Pt nanostructures, namely nanobelts, through the solution-based method. Semiconducting nanobelts, such as zinc oxide (ZnO), tin dioxide (SnO_2) and indium oxide (In_2O_3), have been obtained only in a high-temperature vapor-solid process.[4] Since nanobelts have more well-defined side-surfaces, the energy required for the crystal growth process is generally high; compared to the oxide nanobelts, metal nanobelt is much harder to form which requires reducing environments and the simultaneous shape-control.[5]

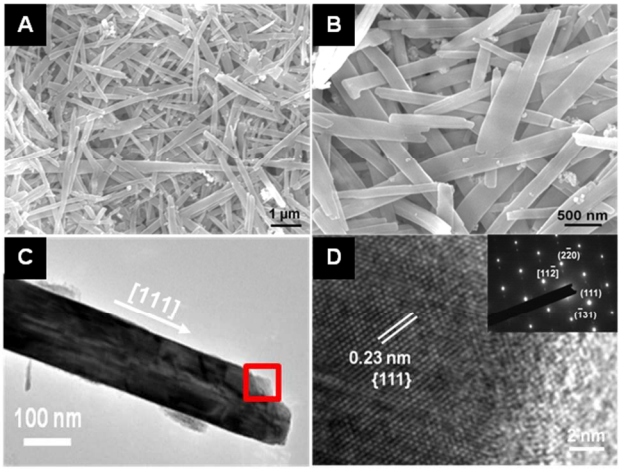

Figure 1. (A, B) SEM and magnified SEM images of the as-synthesized Pt nanobelts. (C) TEM and (D) HRTEM images of the Pt nanobelts taken from the marked area. Inset: SAED pattern of the Pt nanobelt.

Herein we report a solution-based method to synthesize quasi-1D Pt nanobelt structures. The reaction is done via common chemical reagents and in room temperature, which makes the whole process readily scalable. The shape of the nanobelts can be controlled simply by changing the precursor concentration, capping agents, or reaction time. A structural transformation from flat-stacking belts to curved entangled belts was also observed. Compared to other 1-D nanostructures, such as rods, wires or tubes, the quasi-1D nanobelts may have the following advantages: (i) higher conductivity due to well-defined crystalline structure; (ii) better contact/adhesion to the electrodes as a result of the large

portion side-surfaces; (iii) enhanced surface wettability from the unique morphology. These characteristics make the Pt nanobelts especially suitable for electrocatalyst application, where high catalytic activity, rapid electron transport, and good electrode adhesion are the subjects of concern.

The Pt nanobelt was synthesized using a reverse micelle method in a water-in-oil dispersion. Only three steps were involved in the preparation process: (i) 4 mg platinum chloride ($PtCl_2$) was first dispersed in 7 mL toluene by sonication for 5 minutes. Afterwards, 72.89 mg (0.2 mmol) cetrimonium bromide (CTAB) was added into the dispersion and sonicated for 3 minutes. The temperature of the dispersion should be remained at room temperature during the process. The dispersion was then transferred to a hot plate and 0.1 mL ethylenediamine (EDA) was added under constant stirring. (ii) 13 mg sodium borohydride ($NaBH_4$) was dissolved in 2 mL D.I. water in prior, and then drop-wise added into the dispersion under vigorous stirring. Afterwards, the reaction was allowed to proceed for additional 1 hour. (iii) As the reaction stopped, the organic phase was discarded and the aqueous phase was centrifuged at 3500 rpm after adding 5 mL ethanol. The black precipitation was then repeatedly washed and centrifuged with hot ethanol or water for several times and collected for further characterization.

The morphology of the as-synthesized Pt nanobelt is shown in Fig. 1A, where the belt-shape morphology with sufficient longitudinal and transverse growth can be observed. Shattered belts and extra-long belts are coexisting in the sample images, indicating a relative board length distribution for the nanobelts (around 0.4-5 μm). The surface of the nanobelts is atomic smooth, where few adsorbed amorphous organic sheath or particles are observed; rectangular cross-section can also be observed for the nanobelts (Fig. 1B). Typical TEM image of the nanobelt taken from the near edge area is shown in Fig. 1C. From the corresponding HRTEM image (Fig. 1D), fringe spacing of 0.23 nm can be observed for the nanobelts, indicating the [111] reflection of the Pt crystals. It thus indicates that the Pt nanobelt is a single crystal grown along the [111] direction, which is also supported by the as-obtained SAED pattern. The average length of the nanobelts is 1.85 μm after counting several tens of the belts. Compared to the length, the narrower width distribution is observed for the belts, which is around 120-180 nm. The rectangular cross-section is considered as the unique characteristics of the nanobelts, which is different from the spherical or octagonal cross-section of the nanowires or rods, respectively.[6] The width-to-thickness ratio calculated from the cross-

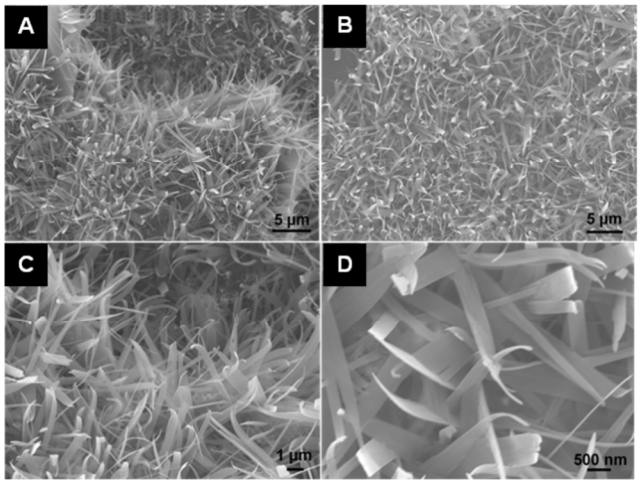

Figure 2. SEM images of the Pt nanobelts obtained in higher Pt salt concentration.

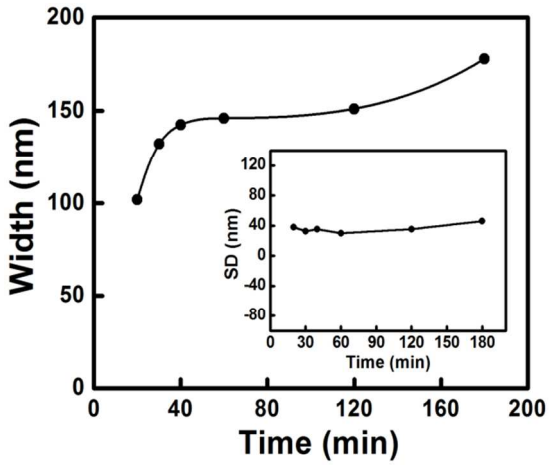

Figure 3. The changing of nanobelt width with increasing reaction time (20, 30, 40, 60, 120 and 180 min). Inset: standard deviation (SD) of the width calculated from the sample obtained at different reaction time.

sectional dimensions is also an important factor for defining the shapes of the nanobelts. However, the Pt nanobelts have the width-to-thickness ratio around 2-4, which are smaller than the oxide nanobelts.[7] Fig. S1 shows a typical cross-sectional view of the nanobelts, from which a wide-to-thickness ratio of 4 can be observed. Small shape deviation from rectangular is also observed, due to the high surface energy of the facets at the ends. The peaks in the XRD pattern of the Pt nanobelt can be indexed to the (111), (200), (220), (311), (222) crystal planes of platinum, indicating the belts are in the face-center-cubic (*fcc*) crystalline structure, which is similar to the bulk Pt (Fig. S2).[8]

The shape of the Pt nanobelts can be easily controlled by adjusting the Pt salt precursor concentration. Upon increasing the amount of added $PtCl_2$ to 16 mg, well-defined curved nanobelts were obtained (Figure 2A). The length of the curved nanobelts is distributed around 1.5-6 μm, with an average length of 4 μm; on the other hand, the width of these belts is around 0.2-1 μm, with an average of 470 nm, after counting several tens of the belts. It is clear to observe that the curved Pt nanobelts have homogeneous shape distribution (Figure 2B), while the crystals start to tilt and curve at the tips (Figure 2C), assembling the nature petals. Compared to the flat nanobelts synthesized previously, these curved nanobelts are more "compressed", which means they are wider and thinner, as shown in Figure 2D. Larger width-to-thickness ratio is observed for the curved belts, which is in the range of 4-12. However, the curved nanobelts are generally larger than the flat belts in terms of width

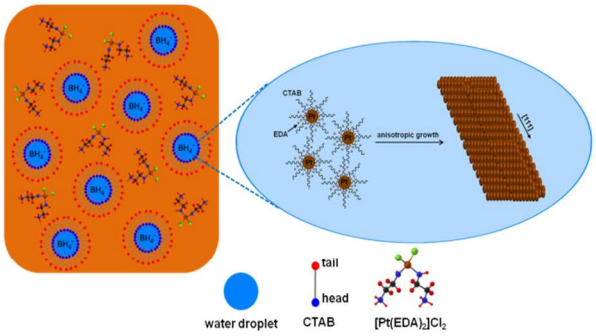

Scheme 1. Formation steps of Pt nanobelts.

and length. According to the increased $PtCl_2$ concentration, the transformation from the flat-stacking nanobelts to curved entangled belts can be largely attributed to the enhanced saturation ratio during the reaction.[9] With excess Pt source existed in the solution, the flat nanobelts then continue to grow into larger curved belts with more uniform shapes through a self-sharpening process,[10] even though the size of the irregular shape by-products is also increased. The width of the flat nanobelts can be further controlled by changing the reaction time. The average width is changing from 102 nm to 178 nm as the reaction time increase from 20 min to 3 h whilst the other parameters are kept constant (Figure 3). The nearly constant standard deviation (SD) of the sample width for each time-slot (Figure 3: inset) indicates that the synthesis process is readily controllable and the width of the belts is determined by the reaction time under the given condition.

CTAB and EDA are indispensable for the formation of Pt nanobelts as without the addition of each of these two reagents, only nanoparticle aggregates are obtained. It is believed that the Pt nanobelts were formed through a reverse micelle micro-reaction mechanism (Scheme 1). Small water droplets were dispersed by CTAB in toluene while the solution was vigorously agitated. These water droplets contained $NaBH_4$ can then extract the Pt^{2+} ions from the organic phase. As the Pt^{2+} entered the water droplet, it was quickly reduced into Pt^0 by $NaBH_4$ and formed nuclei to support further growth.[11] At this time, the water droplets served as the micro-reactors for the crystal growth to occur. The preference adsorption of the surfactant and capping agents, i.e. CTAB and EDA onto the growing facets would induce the anisotropic 1-D growth of the Pt nuclei.[12] In case of Pt and Pd, it has also been widely reported that the capping effect is preferred to take place on the {110} facet, resulting in the directional [111] growth.[13] On the other hand, the chelating effect of EDA on Pt^{2+} ions formed charged complexes, i.e.

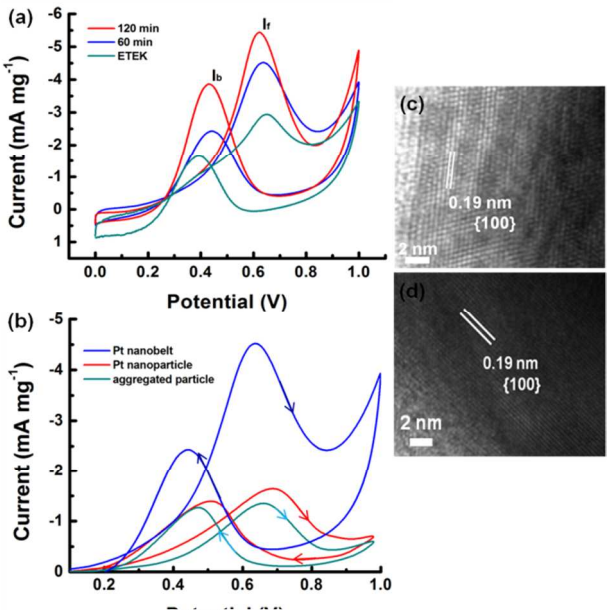

Fig. 4 (a) Cyclic voltammograms (CVs) of Pt nanobelt obtained at 120 min (red), 60 min (blue) and ETEK catalyst (green) in 0.5M MeOH/0.5M H_2SO_4 solution. (b) CVs of Pt nanobelt, Pt nanoparticle synthesized without CTAB and aggregated Pt particles without the addition of CTAB and EDA in 0.5 M MeOH/0.5 M H_2SO_4 solution. Scan rate: 50 mV s^{-1}. (c, d) HRTEM images of the as-synthesized Pt nanoparticles and aggregated Pt particles, respectively.

$[Pt(EDA)_2]^{2+}$.[14] The steric hindrance and charge interaction of the complex to the growing plane thus induced the radial expansion of the side surface, resulted in a quasi-1D structure with rectangular cross-section.[15] This phenomenon was also observed when using EDA as the capping agent to synthesize 1D Cu nanostructure, as quasi-1D Cu nanoflakes with expanded side-surface were also formed (Fig. S3).

The well-defined crystalline structure and flat side-surface make the Pt nanobelt ideal for electrocatalyst applications. The Pt belts were dispersed in Nafion and casted on glassy carbon electrode for the electrochemical (EC) methanol oxidation reaction (MOR). The nanobelts synthesized in 60 min, 120 min and the ETEK commercial catalyst were used for comparison (Figure 4). Characteristic methanol oxidation peaks centered around +0.65 V (I_f, anodic scan) and +0.45 V (I_b, cathodic scan) can be observed for the three electrocatalysts.[15] Higher I_f current density can be observed for the Pt nanobelts (60 min, 120 min) compared to the ETEK catalyst, indicating higher catalytic activity to MOR for the nanobelts. The catalytic activity of the electrode is affected by different belt morphologies. The nanobelt synthesized in 120 min (avg. width = 151 nm) shows higher oxidation current density and lower CO tolerance with a I_f/I_b ratio of 1.41;[16] while the belt synthesized in 60 min (avg. width = 146 nm) shows lower current density and a higher CO tolerance (I_f/I_b = 1.86). Better CO tolerance may rise from the higher surface area of smaller belts. On the other hand, it also reveals controlled properties of the nanomaterial and enhanced system efficiency can be realized by acute nanoscale engineering.

Control experiments were also performed by synthesizing Pt nanoparticles and aggregated Pt particles without adding CTAB or both CTAB/EDA, respectively. It can be observed from the TEM images that the as-synthesized Pt nanoparticles generally obtained a size around 50 nm, while the size of the aggregated Pt particles varies, from several hundreds of nanometers to micron (Fig. S4). However, the Pt nanoparticle and aggregated particle also showed catalytic activities to MOR, which inferior to the nanobelts to a large extent, in terms of the current density and I_f/I_b ratio (Fig. 4a). Mainly Pt(100) surface atoms were observed for the as-synthesized Pt nanoparticles (Fig. 4c) and aggregated particles (Fig. 4d), indicating a different surface composition to the Pt nanobelt structure. With the Pt(111) facets exposing on the surface, the Pt nanobelt has obtained much higher electrocatalytic activity compared with the Pt(100) surface particles. It has also been widely reported that the Pt(111) would have the highest catalytic property among the facets due to its relatively low activation energy.[18] Nonetheless, this preferential facet control over the anisotropic nanobelt structure can also benefit the electrocatalytic application to a large extent.

Using our method, novel Pt nanobelt with controlled shape and size can be obtained in solution for the first time. Upon changing the parameters, i.e. concentration and time, the morphology of the nanobelt can be transformed from the flat-stacking belts to the curved entangled belts; and the width of the nanobelt can also be controlled. The nanoscale engineering on the morphologies of the belts has enabled acute control on their electrocatalytic properties, as the MOR activity and CO tolerance of the belts can be tuned by changing the width. Therefore this controlled nanobelt system is quite attractive for the electrocatalyst applications. Bringing about the intrinsic high conductivity, electrode contact, high wettability and tunable EC properties of the nanobelts, they can probably serve as the important building blocks for fuel cells, sensors and catalyst in the future.

The authors gratefully acknowledge the financial support from the U.S. NSF (CMMI-1000491) grant and The Hong Kong Polytechnic University.

Notes and references

[a] Department of Polymer and Fiber Engineering, Auburn University, Auburn, AL 36849, USA, Fax:1-334-844-4068; Tel:1-334-844-5439; E-mail:xzz0004@auburn.edu.
[b] Nanotechnology Centre, The Hong Kong Polytechnic University, Hung Hom, Kowloon, Hong Kong (Current affiliation of the first author).
† Electronic Supplementary Information (ESI) available: experimental details, SEM, TEM images, TGA and CV of the Pt nanobelts. See http://dx.doi.org/10.1039/b000000x/

1 a) C. Burda, X. Chen, R. Narayanan, M. A. El-Sayed, Chem. Rev. 2005, 105, 1025-1102; b) R. S. Devan, R. A. Patil, J. H. Lin, Y. R. Ma, Adv. Funt. Mater. 2012, 22, 3326-3370; c) M. Cain, R. Morrell, Appl. Organomet. Chem. 2001, 15, 321-330.
2 A. Chen, P. H. Hindle, Chem. Rev. 2012, 110, 3767-3804.
3 a) K. Kim, K. L. Kim, H. B. Lee, K. S. Shin, J. Phys. Chem. C 2010, 114, 18679-18685; b) J. K. Kawasaki, C. B. Arnold, Nano. Lett. 2011, 11, 781-785; c) T. S. Zhao, Z. X. Liang, J. Phys. Chem. C 2007, 111, 8128-8134.
4 Z. L. Wang, Annu. Rev. Phys. Chem. 2004, 55, 159-196.
5 D. L. Ma, H. L. Chen, Cryst. Growth Des. 2009, 9, 2030-2035.
6 a) Y. Song, R. M. Garcia, R. M. Dorin, H. Wang, Y. Qiu, E. N. Coker, W. A. Steen, J. E. Miller, J. A. Shelnutt, Nano. Lett. 2007, 7, 3650-3655; b) H. K. Boon, C. J. Rossouw, M. Weyland, A. M. Funston, P. Mulvaney, J. Etheridge, Nano. Lett. 2011, 11, 273-278.
7 Z. W. Pan, Z. R. Dai, Z. L. Wang, Science 2001, 291, 1947-1949.
8 X. Fu, Y. Wang, N. Wu, L. Gui, Y. Tang, J. Mater. Chem. 2003, 13, 1192-1195.
9 C. B. Murray, C. R. Kagan, M. G. Bawendi, Annu. Rev. Mater. Sci. 2000, 30, 545-560.
10 Q. Zhang, S. J. Liu, S. H. Yu, J. Mater. Chem. 2009, 19, 191-207.
11 H. C. Brown, C. A. Brown, J. Am. Chem. Soc 1962, 84, 1493-1494.
12 B. D. Busbee, S. O. Obare, C. J. Murphy, Adv. Mater. 2003, 15, 414-416.
13 M. J. Carter, J. K. Beattie, Inorg. Chem. 1970, 9, 1233-1238.
14 Y. Chang, M. L. Lye, H. C. Zeng, Langmuir 2005, 21, 3746-3748.
15 Y. Liu, N. Lu, S. Poyraz, X. Wang, Y. Yu, J. Scott, J. Smith, M. J. Kim, X. Zhang, Nanoscale 2013, 5, 3872-3879.
16 Y. Mu, H. Liang, J. Hu, L. Jiang, L. Wan, J. Phys. Chem. B 2005, 109, 22212-16.

